



Photochemical production of ammonium in the oligotrophic Cyprus Gyre (Eastern Mediterranean)

V. Kitidis, G. Uher, R. C. Upstill-Goddard, R. F. C. Mantoura, G. Spyres, E. M. S. Woodward

► **To cite this version:**

V. Kitidis, G. Uher, R. C. Upstill-Goddard, R. F. C. Mantoura, G. Spyres, et al.. Photochemical production of ammonium in the oligotrophic Cyprus Gyre (Eastern Mediterranean). Biogeosciences, European Geosciences Union, 2006, 3 (4), pp.439-449.

HAL Id: hal-00297575

<https://hal.archives-ouvertes.fr/hal-00297575>

Submitted on 9 Oct 2006

HAL is a multi-disciplinary open access archive for the deposit and dissemination of scientific research documents, whether they are published or not. The documents may come from teaching and research institutions in France or abroad, or from public or private research centers.

L'archive ouverte pluridisciplinaire **HAL**, est destinée au dépôt et à la diffusion de documents scientifiques de niveau recherche, publiés ou non, émanant des établissements d'enseignement et de recherche français ou étrangers, des laboratoires publics ou privés.

Photochemical production of ammonium in the oligotrophic Cyprus Gyre (Eastern Mediterranean)

V. Kitidis^{1,*}, G. Uher¹, R. C. Upstill-Goddard¹, R. F. C. Mantoura^{2,**}, G. Spyres², and E. M. S. Woodward²

¹Ocean Research Group, School of Marine Science and Technology, University of Newcastle upon Tyne, Newcastle upon Tyne, NE7 7RU, UK

²Plymouth Marine Laboratory, Plymouth, PL1 3DH, UK

* now at: Plymouth Marine Laboratory, Plymouth, PL1 3DH, UK

** now at: International Atomic Energy Authority Marine Ecology Laboratory, Monaco

Received: 7 March 2006 – Published in Biogeosciences Discuss.: 1 June 2006

Revised: 23 August 2006 – Accepted: 5 October 2006 – Published: 9 October 2006

Abstract. We investigated the photoproduction of ammonium (NH_4^+) in surface waters of the Cyprus gyre in the central Eastern Mediterranean in May 2002, in 8 on deck irradiations with freshly collected, filtered samples. NH_4^+ photoproduction (photoammonification) increased with time-integrated irradiance during the course of irradiations. Photoammonification rates around local noon were $0.4\text{--}2.9\text{ nmol L}^{-1}\text{ h}^{-1}$. Normalised to time integrated irradiance, these rates were $0.9\text{--}3.8\text{ pmol L}^{-1}\text{ h}^{-1}/(\text{W m}^{-2})$ and were significantly correlated with Chromophoric Dissolved Organic Matter (CDOM) absorbance at 300 nm normalised to Dissolved Organic Carbon (DOC). These results are consistent with the notion that successive CDOM photobleaching in the surface mixed layer results in decreased DOC-normalised light absorbance concurrent with decreased dissolved organic matter reactivity with regard to photochemical NH_4^+ release. Combining our experimental data with estimates of annual solar irradiance and water column light attenuation yields an annual photoammonification rate for the Cyprus Gyre of $40\pm 17\text{ mmol m}^{-2}\text{ a}^{-1}$, equivalent to $\sim 12\pm 5\%$ of the previously estimated annual nitrogen requirement of new production and in the same order of magnitude as atmospheric N deposition in this region. Based on this analysis, NH_4^+ photoproduction makes a small, but significant contribution to the nitrogen budget of the euphotic zone in the oligotrophic Cyprus Gyre.

1 Introduction

Photoproduction of ammonium (NH_4^+) via the photodegradation of chromophoric dissolved organic matter (CDOM) can significantly modify the inorganic nutrient budgets of aquatic ecosystems (Bushaw et al., 1996). The reaction mechanisms involved are unknown, but several pathways are thought to exist involving photochemical reactions between ketones and aldehydes with amines to form a Schiff base that is hydrolysed to release NH_4^+ (Bushaw et al., 1996) and NH_4^+ release through hydrolysis of CDOM-photosensitised amino acids (Tarr et al., 2001). Recent evidence indicates that the impacts of photochemical NH_4^+ release may vary considerably between distinct biogeographic settings. Bushaw et al. (1996) estimated photoproduction of NH_4^+ (photoammonification) on the Southeastern US continental shelf to contribute an additional 20% to riverine inorganic nitrogen export. Similarly, Morell and Corredor (2001) estimated the contribution of NH_4^+ photoproduction to the phytoplankton nitrogen (N) demand of the eastern Caribbean Sea at $\sim 50\%$. In contrast, Buffam and McGlathery (2003) found that the contribution of photoammonification to the N sources of a coastal lagoon was small compared to other inputs. These observations seem to suggest that the potential impact of photoammonification is highest in shelf waters and marginal seas. However, the role of photochemistry in open ocean nutrient budgets has received little attention, even though NH_4^+ photoproduction may represent a significant source of N for primary producers in N-depleted surface waters of the open ocean.

Recent work provides growing evidence for significant photoammonification rates particularly in inland, estuarine and coastal waters with elevated DOM levels. Photoammonification rates of up to $220\text{ nmol L}^{-1}\text{ h}^{-1}$ were observed in

Correspondence to: V. Kitidis
(vak@pml.ac.uk)

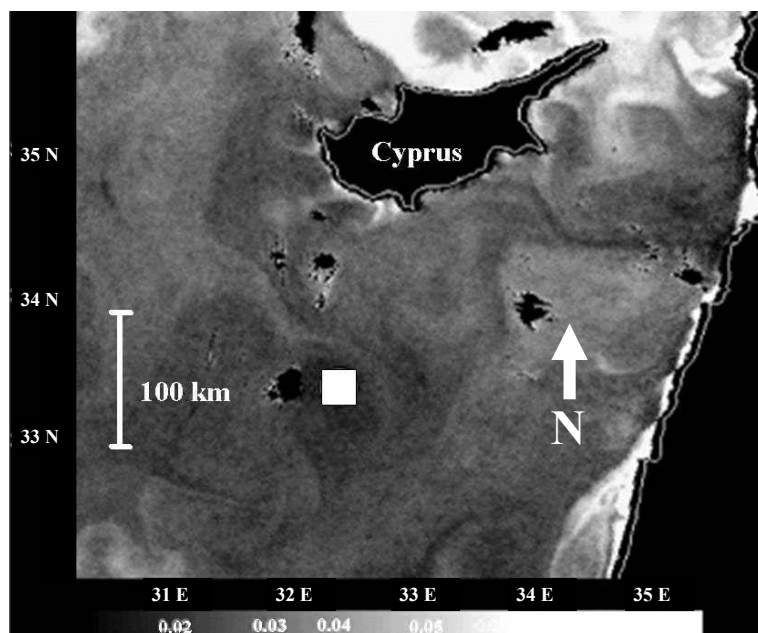


Fig. 1. Composite ocean colour image of the Eastern Mediterranean showing location of the study area (white square). Image courtesy of Plymouth Marine Laboratory Remote Sensing Data Analysis Service with SeaWiFS data from NASA and Orbimage Inc.

estuarine and coastal seawater (Bushaw et al., 1996; Gardner et al., 1998; Bushaw-Newton and Moran, 1999; Morell and Corredor, 2001; Koopmans and Bronk, 2002; Buffam and McGlathery, 2003), while rates of up to $4700 \text{ nmol L}^{-1} \text{ h}^{-1}$ (corrected for dilution during ultrafiltration), were observed in freshwaters (Bushaw et al., 1996; Gao and Zepp, 1998; Wang et al., 2000; Koopmans and Bronk, 2002; Buffam and McGlathery, 2003; Vähätalo et al., 2003). In addition to ammonium, photoproduction of nitrite (NO_2^-) and low molecular weight organic nitrogen compounds such as dissolved primary amines and dissolved free amino acids were also observed (Spokes and Liss, 1996; Bushaw-Newton and Moran 1999; Kieber et al., 1999; Tarr et al., 2001; Wiegner and Seitzinger, 2001; Koopmans and Bronk, 2002; Buffam and McGlathery, 2003). However, the associated photoproduction rates of these N compounds are generally one order of magnitude lower than corresponding rates of photoammonification. Net NH_4^+ photoproduction is nevertheless not ubiquitous. Several studies were unable to detect photoammonification during irradiations of lake and river waters (Jørgensen et al., 1998; Bertilsson et al., 1999; Wiegner and Seitzinger, 2001). Photoammonification rates must therefore be considered in their regional context and in comparison with other N sources in order to assess their importance.

The contrasting observations of high nutrient photoproduction rates in some regions as compared to low or undetectable rates in others most likely reflect not only regional variability in DOM reactivity, but also the effects of various environmental controls that are not well understood. For example, Wang et al. (2000) report pH control of photoam-

monification in river and estuarine waters, and Gao and Zepp (1998) observed that the presence of dissolved iron (Fe) enhanced photoammonification rates in river water. Net photochemical uptake of NH_4^+ by DOM has also been observed both in C18 extracted dissolved organic matter (DOM) of marine- (Kieber et al., 1997) and in filtered brackish- (Gardner et al., 1998) and ground-waters (Koopmans and Bronk, 2002). Additional controls of photoammonification suggested in published work include intrinsic DOM properties, ambient oxygen levels, and prior radiation exposure (Koopmans and Bronk, 2002; Buffam and McGlathery, 2003). While some of the variability in photochemical NH_4^+ production rates may be plausibly explained by combinations of these aforementioned controls, regional extrapolations of NH_4^+ photoproduction remains challenging, nonetheless because of significant gaps in data coverage.

Currently published data on photoammonification are heavily biased towards freshwater, estuarine and coastal studies and consequently data from open ocean areas characterised by low ambient inorganic N levels under stratified conditions are lacking. To our knowledge there exists only one report of oceanic photoammonification rates from the Eastern Tropical Pacific (Bronk, 2002). Although the rates reported by Bronk (2002) indicate a potentially important role for this process in the open ocean, they are lacking further information such as details on local hydrography, productivity regime, and CDOM, which are needed to assess their potential importance. Additional oceanic estimates are therefore required, especially in view of the difficulties associated with extrapolating data from freshwaters or

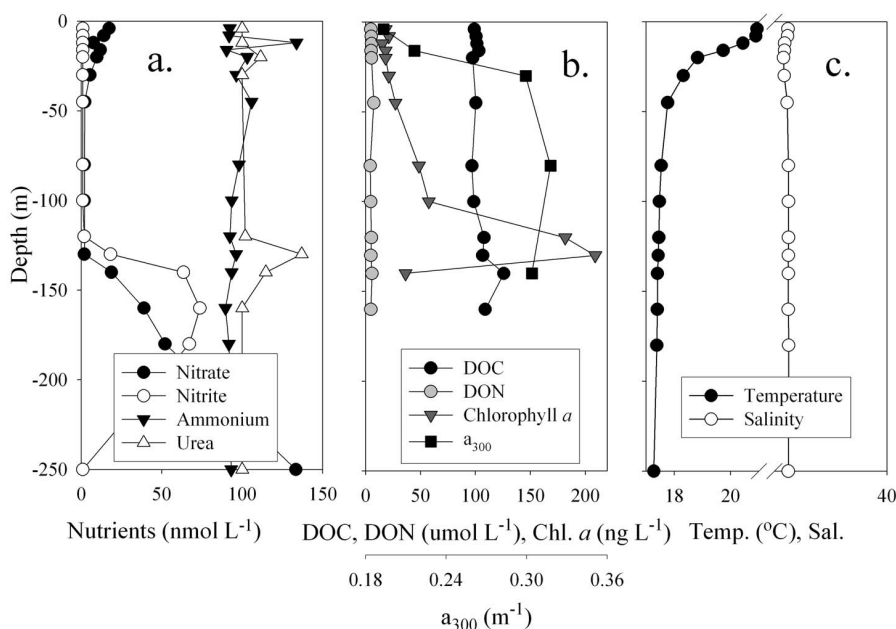


Fig. 2. The depth distribution of (a) NO_3^- , NO_2^- , NH_4^+ , urea, (b) DOC, DON, CDOM (a_{300}), Chlorophyll a and (c) temperature and salinity for a typical example of a post-release station (2CYC27).

coastal seas, such as the possibility of photoammonification inhibition at typical seawater pH (Buffam and McGlathery, 2003), and modification of the photoammonification potential of CDOM through prior radiation exposure in clear open ocean waters.

One ocean region in which photochemical processes could significantly impact nutrient budgets is the Eastern Mediterranean Sea, which is characterised by low ambient inorganic N levels, typical of oligotrophic waters (Rees and Woodward, 1999) and unique in showing proximate P-limitation (Krom et al., 1991, 1992, 2004). Recent work in the Cyprus Gyre of the central Eastern Mediterranean has shown that while the heterotrophic microbial community remains P limited during summer, phytoplankton are N and P co-limited (Krom et al., 2005a; Thingstad et al., 2005). Hence photoproduction of N in the Eastern Mediterranean could have significant implications for regional net productivity.

In this study we conducted a series of sunlight irradiations in surface waters of the Cyprus Gyre. We determined photoproduction rates of NH_4 and combined these with estimates of annual solar irradiance and light attenuation in order to assess the photochemical contribution to the annual nutrient budget of this region.

2 Methods

2.1 Study area

On-deck irradiation experiments were carried out during cruise CYC2 of RV *Aegaeo*, in the Cyprus gyre

during May 2002 (Fig. 1). The central cruise objective was to carry out a Lagrangian experiment involving a dual PO_4^{3-} - SF_6 tracer release (Law et al., 2005), an integral component of the EU-CYCLOPS program (<http://www.earth.leeds.ac.uk/cyclops/>). In brief a 4×4 km patch of surface water located in the core of an anticyclonic eddy centred on 33.3°N , 32.3°E , was infused with PO_4^{3-} and SF_6 . SF_6 (sulphur hexafluoride) is an anthropogenic gas that was used as an inert tracer of physical processes (patch dilution through lateral advection) in this instance. The patch was released on the 17 May 2002 and subsequent changes in a range of biogeochemical parameters were followed over a 9 day period at IN-patch stations and compared to pre-release and OUT-patch stations at a minimum distance of 15 km from the patch centre. An overview of procedural details and results was published elsewhere (Krom et al., 2005a).

The hydrography and N-biogeochemistry of the study area is described in detail by Krom et al. (2005b) and is briefly reviewed here. Figure 2 shows the depth distribution of NO_3^- , NO_2^- , NH_4^+ , urea, DOC, DON, CDOM (a_{300}), Chlorophyll a , temperature and salinity for a typical example of a post-release station (2CYC27). A 200 m deep, nutrient depleted surface mixed layer was found with a secondary, shallow (seasonal) thermocline at approximately 20 m depth. The mixed layer salinity was ~ 39.1 and its temperature was 17–20°C. Surface mixed layer chlorophyll a levels were in the range of 20–50 ng L^{-1} . A deep chlorophyll a maximum (DCM) of 200 ng L^{-1} was located at approximately 110 m. The primary NO_2^- maximum was observed between 130–160 m and was associated with the pycnocline. NH_4^+ concen-

Table 1. Initial properties of irradiated samples; a_{300} (m^{-1}), DOC ($\mu\text{mol L}^{-1}$) and photoammonification rate ($\text{pmol L}^{-1} \text{h}^{-1}/(\text{W m}^{-2})$) normalised to time-integrated irradiance (non-normalised rate in brackets, $\times 10^3 \text{pmol L}^{-1} \text{h}^{-1}$). Samples were classified according to their origin into: a) Deep Chlorophyll Maximum (DCM) and b) IN- and c) OUT- stations in relation to the $\text{PO}_4^{3-}/\text{SF}_6$ patch. Time refers to days pre- (negative) and post-release (positive) of the $\text{PO}_4^{3-}/\text{SF}_6$ patch.

IREX	Time	Station	a_{300}	DOC	Photoammonification
1	-1.5	DCM	0.25	51	3.8 (2.9)
2	0.5	DCM	0.36	109	1.9 (1.5)
3	1.5	IN-20 m	0.26	110	0.9 (0.7)
4	3.5	IN-20 m	0.22	62	2.8 (2.2)
5	3.5	IN-30 m	0.26	62	1.6 (1.2)
6	5.5	IN-20 m ($>360 \text{nm}$)	0.26	77	2.1 (1.6) 0.5 (0.4)
7	5.5	IN-20 m	0.22	77	1.5 (1.2)
8	6.5	OUT-20 m	0.19	77	2.1 (1.6)
mean			0.25	78	2.1 (1.6)

tration in the surface mixed layer was 30–140 nmol L^{-1} . The depth distribution of NH_4^+ showed a pronounced maximum at the base of the seasonal thermocline ($\sim 30 \text{m}$) and a less pronounced maximum in the vicinity of the primary nitrite maximum (Fig. 2). Dissolved Organic Nitrogen (DON) in the surface mixed layer was in the range of 5–10 $\mu\text{mol L}^{-1}$. Urea, determined according to Goyens et al. (1998) for only one in-patch station (2 days post release, station 2CYC27), showed a concentration maximum of 140 nmol L^{-1} at ~ 120 –140 m depth and otherwise remained below analytical detection limits ($<100 \text{nmol L}^{-1}$).

2.2 Sampling and sunlight irradiations

In total, 8 irradiation experiments (IREX) were carried out with water samples from the DCM, surface IN-patch and surface OUT-patch. Sample details are listed in Table 1. Water samples for irradiation experiments ($\sim 10 \text{L}$) were collected daily between 8 am and 10 am local time using a CTD-rosette sampler and filtered immediately ($0.1 \mu\text{m}$, Whatman, Polycap 75TF). Filtrates were collected in 20 L polyethylene carboys, pre-cleaned with dilute HCl and analytical grade water (Millipore, model Milli-Q 185, hereinafter referred to as Milli-Q). Samples were stored in the dark at room temperature until irradiation the following day. Each sample was used to completely fill a series of cylindrical quartz irradiation flasks with an internal volume of 430 mL. These were then immediately capped with Nylon compression fittings (SwagelokTM) and placed in a shallow deck incubator, which was continuously flushed with ambient surface seawater. The irradiations ran for $\leq 3 \text{h}$ around local solar noon, with sequential sampling for dissolved NH_4^+ . Dark control flasks

were treated identically, except that they were wrapped in double aluminium foil to exclude light. All irradiations were carried out within 30 h of sample collection. We assumed storage artefacts to be precluded by this protocol, as in previous work 45 day dark storage of $0.2 \mu\text{m}$ filtered coastal water did not affect subsequent rates of NH_4^+ photoproduction (Morell and Corredor, 2001). Flow cytometry of selected samples confirmed the removal of $>99.5\%$ of bacteria and picoplankton by our filtration protocol (M. Zubkov, personal communication).

Samples for dissolved organic carbon (DOC) and nitrogen (DON) were collected daily from the CTD-rosette sampler. Polythene (powder-free) gloves were worn throughout handling procedures. Pre-cleaned all-glass syringe systems with Teflon tubing and an on-line stainless-steel unit containing $0.7 \mu\text{m}$ glass fibre filter (Whatman, GF/F) were used to collect the water samples directly from the CTD bottle. Filters were pre-combusted in an oven at 450°C for at least 4 h. The samples were transferred to pre-combusted 10 mL glass ampoules, acidified with high-grade phosphoric acid and flame sealed. The glass ampoules containing the sample were stored cold ($\sim 4^\circ\text{C}$) in the dark and transferred for analysis on-shore.

Global solar irradiance was measured continuously with the ship's solar radiation sensors (Aandera Instruments, Solar Radiation Sensor model 2770) and recorded as 10 min averages throughout the entire cruise. Mean global solar irradiance during the experiments was $842 \pm 95 \text{W m}^{-2}$. In one irradiation experiment a sample subset was screened with a clear acrylic sheet (10% transmission at 360 nm) in order to investigate the broadband wavelength dependence of NH_4^+ photoproduction. A broadband UV sensor (Delta-T, model UV-AB) showed that approximately 50% of the ambient UV light ($<400 \text{nm}$) passed through the acrylic filter.

2.3 Sample analysis

Nanomolar NH_4^+ was determined by flow injection analysis with fluorometric detection, following preconcentration by diffusion across a microporous hydrophobic membrane and derivatisation with *o*-phthal-dialdehyde (OPA) (Jones, 1991). Fresh standards were prepared daily in low nutrient seawater, which was collected previously in the surface central North Atlantic, filtered through a $0.2 \mu\text{m}$ filter and aged in the dark for ~ 12 months. The detection limit ($2 \times$ standard deviation of the blank) was 1nmol L^{-1} . The analytical precision was $\pm 2\%$ ($2 \times$ standard deviation of 50nmol L^{-1} standard, $n=6$).

For DOC and DON, samples were analysed by high temperature catalytic oxidation (HTCO) with infrared detection for C (Shimadzu TOC-5000A) and chemiluminescence detection for N (Antek 7000) (Alvarez-Saldago and Miller, 1998; Spyres et al., 2000). Since the HTCO method measures total dissolved nitrogen, we subtracted the concentrations of dissolved inorganic nitrogen (NO_3^- , NO_2^- and NH_4^+) to derive DON data. NO_3^- and NO_2^- were determined ac-

ording to Brewer and Riley (1965) and Grasshoff (1983) respectively. The acidified samples were purged with high purity N₂ gas (BOC gases Ltd.) immediately prior to analysis for approximately 10 min to remove the inorganic carbon. Deep Sargasso seawater samples with a certified DOC concentration of 44.0±1.5 μmol L⁻¹ were used daily as a check on instrument performance and accuracy. Blank correction was applied daily to the DOC measurements.

2.4 CDOM

CDOM absorbance spectra were recorded on a double beam UV-visible spectrophotometer (Shimadzu, model UV 240) at 10 nm intervals between 250 and 800 nm, using 100 mm pathlength quartz cells. Samples were referenced against Milli-Q water and absorbance spectra were corrected for instrument drift by subtracting the mean absorbance for the 650–700 nm wavelength interval (Green and Blough, 1994). This wavelength range was chosen in order to avoid temperature effects on sample absorbance which are confined to slightly longer wavelengths (700–775 nm) (e.g. Pegau and Zaneveld, 1993; Kitidis, 2002). Absorption coefficients were calculated from Eq. (1):

$$a_{\lambda} = \frac{2.303 \times A_{\lambda}}{l} \quad (1)$$

where a_{λ} is the absorption coefficient (m⁻¹) at wavelength λ , A_{λ} is the absorbance at wavelength λ and l is the cell pathlength (m). The absorption coefficient at 300 nm (a_{300}) was used as a proxy for CDOM. Given the detection limit of the spectrophotometer (0.001 absorbance units) and an optical cell pathlength of 0.1 m, the detection limit for CDOM was 0.04 m⁻¹.

2.5 Statistical analysis and precision

All statistical analyses were carried out with Minitab (Minitab Inc., version 13.1). A paired t-test was carried out to explore the significance of differences between the mean a_{300} values and DOC concentrations in surface waters (<30 m) and at depth (>30 m). Both a_{300} and DOC data were normally distributed. Pearson's correlation analysis was used to investigate relationships between photoammonification rate and various environmental parameters. Irradiation of one IN-patch sample was repeated on two consecutive days (IREX 6 and 7) in order to assess the overall precision of our experimentally derived rate data.

3 Results

3.1 Initial sample properties

An initial survey of the study area established the mixed layer distributions of CDOM (a_{300}), DOC and DON (Table 2). CDOM was the main UV absorbing chromophore in surface

Table 2. Average (±standard deviation) CDOM, DOC, DON and DOC:DON ratio in near-surface water (0–30 m) and deeper water (30–1600 m) of the study area. Significant differences (t-test) between depth intervals are denoted *: $p < 0.01$ and **: $p < 0.001$.

Depth	0–30 m	30–1600 m
CDOM (a_{300} , m ⁻¹) *	0.25±0.04 ($n=46$)	0.29±0.06 ($n=22$)
DOC (μmol L ⁻¹) **	88±16 ($n=66$)	76±23 ($n=90$)
DON (μmol L ⁻¹)	4.7±1.9 ($n=89$)	4.2±2.1 ($n=97$)
DOC : DON	18.7	18.1

waters of the Cyprus Gyre due to low ambient concentrations of NO₃⁻ and NO₂⁻ (<10 nmol L⁻¹, Krom et al., 2005b). The near-surface (0–30 m) mean a_{300} (±standard deviation) was 0.25±0.04 m⁻¹ (range: 0.14–0.36 m⁻¹, $n=46$) and the respective mean a_{300} (±standard deviation) in deeper water (30–1600 m) was 0.29±0.06 m⁻¹ (range: 0.16–0.45 m⁻¹, $n=22$). These means were significantly different (t-test, $p < 0.01$, degrees of freedom: 30), with lower CDOM absorbance in near-surface waters.

The near-surface (0–30 m) mean DOC (±standard deviation) was 88±16 μmol L⁻¹ (range: 60–123 μmol L⁻¹, $n=66$) and the respective mean DOC (±standard deviation) in deeper water (30–2600 m) was 76±23 μmol L⁻¹ (range: 37–126 μmol L⁻¹, $n=90$). The respective means were significantly different (t-test, $p < 0.001$, degrees of freedom: 152), with higher DOC concentrations in near-surface waters. Near surface (<30 m) DOM therefore had lower absorbance per unit carbon than DOM in deeper water (>30 m).

The near-surface (0–30 m) mean DON (±standard deviation) was 4.7±1.9 μmol L⁻¹ (range: 1.2–11.1 μmol L⁻¹, $n=89$) and the respective mean DON (±standard deviation) in deeper water (30–2600 m) was 4.2±2.1 μmol L⁻¹ (range: 0.3–12.3 μmol L⁻¹, $n=97$). In contrast to the observed differences in CDOM and DOC, the respective DON means over the two depth intervals were not significantly different (t-test, $p=0.152$, degrees of freedom: 179). These findings indicate that DOC and DON did not co vary with each other over the depth range investigated. The mean DOC:DON ratio in near-surface water (0–30 m) was 18.7 and only slightly above that of deeper water (30–2600 m), which was 18.1. Our data therefore indicate only small differences in DON concentrations and DOC:DON ratios between surface and depth. It is, however, possible that the high variability of DON concentrations within each depth interval may have masked statistically significant compositional differences.

All samples subsequently used in irradiation experiments had initial a_{300} and DOC values within the respective ranges of surface and deep water (Table 1). Hence we considered the irradiated samples to be representative of the study area.

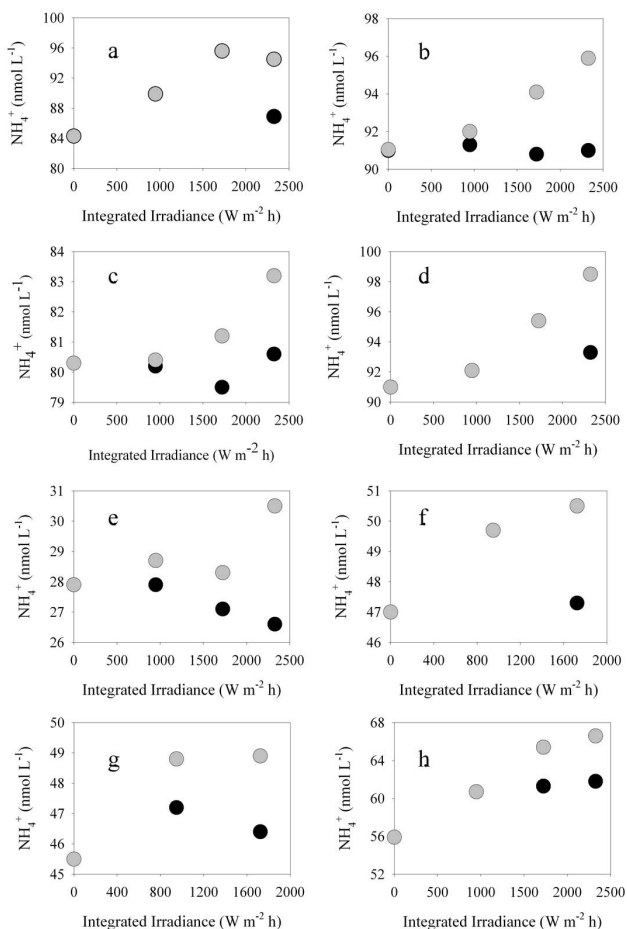


Fig. 3. Ammonium concentration in irradiated samples (grey circles) and dark controls (black circles) in IREX1-8: a–h. The scale of the y-axis differs between panels a–h.

3.2 Irradiations

Figure 3 shows changes in NH_4^+ concentration against time-integrated light intensity during individual irradiation experiments. Dark controls are also shown. In all irradiations NH_4^+ increased with time or time-integrated irradiance, while the NH_4^+ concentration in dark controls showed little variability, remained largely unchanged within analytical precision, and always lower than corresponding NH_4^+ concentrations in irradiated samples (Fig. 3). Irradiance normalised photoproduction rates were determined from the slope of the linear regression of NH_4^+ concentration against time-integrated irradiance over the course of each experiment for light treated samples. In order to correct for any non-photochemical changes, the slope of the respective regression for dark controls was subtracted in each case. Photoammonification rates obtained in this way were in the range of 0.9–3.8 $\text{pmol L}^{-1} \text{h}^{-1}/(\text{W m}^{-2})$ (Table 1). The mean (\pm standard deviation) of photoammonification rates normalised to light intensity was $2.1 \pm 0.9 \text{ pmol L}^{-1} \text{h}^{-1}/(\text{W m}^{-2})$. The preci-

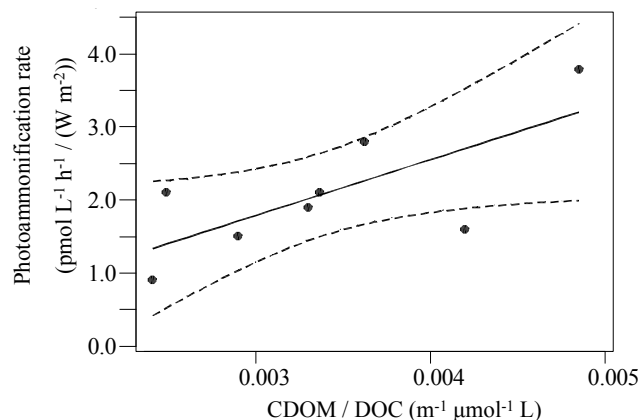


Fig. 4. Irradiance normalised photoammonification rates against DOC normalised CDOM. Linear regression (solid line) and 95% confidence intervals (dashed lines) are shown.

sion of these rate data, defined as the standard deviation of the rates calculated from duplicate rate determinations (IREX 6 and 7) was $0.4 \text{ pmol L}^{-1} \text{h}^{-1}/(\text{W m}^{-2})$. During IREX 1, an irradiated flask was kept in the dark for 2 h before NH_4^+ concentration analysis, following a 2.5 h irradiation period and then compared to a sample analysed immediately after the end of the 2.5 h irradiation. This was done in order to examine potential post-irradiation dark uptake of photoproduced NH_4^+ or continued production of NH_4^+ in the dark. We found no discernible NH_4^+ concentration change post-irradiation and therefore concluded that NH_4^+ released during this experiment was not reincorporated into dissolved organic nitrogen (DON) or otherwise removed. In IREX 6, the photoammonification rate in the sample subset exposed to light $>360 \text{ nm}$ was only $0.5 \text{ pmol L}^{-1} \text{h}^{-1}/(\text{W m}^{-2})$ compared to $2.1 \text{ pmol L}^{-1} \text{h}^{-1}/(\text{W m}^{-2})$ for the subset exposed to the full solar spectrum. This indicated that UV light of wavelengths below 360 nm accounted for 76% of NH_4^+ photoproduction during this irradiation.

Overall, photoammonification rates were not correlated with either CDOM (a_{300}) or DOC alone, but were significantly correlated with CDOM normalised DOC (Pearson correlation coefficient $R^2=0.52$, $p < 0.05$, $n=8$) (Fig. 4). There was no apparent change with time in the photoammonification rate of surface IN-patch samples following the release of the $\text{PO}_4^{3-}/\text{SF}_6$ patch. Furthermore, photoammonification rates were $1.8 \pm 0.4 \text{ pmol L}^{-1} \text{h}^{-1}/(\text{W m}^{-2})$ in IN-patch water 5.5 days after the patch release and $2.1 \text{ pmol L}^{-1} \text{h}^{-1}/(\text{W m}^{-2})$ in OUT-patch water 6.5 days after release. Therefore, we concluded that the addition of PO_4^{3-} to surface waters of the Cyprus Gyre had no effect on photoammonification rates over the short period studied.

Table 3. Published NH_4^+ production rates ($\text{nmol L}^{-1} \text{h}^{-1}$) in freshwater, estuarine (salinity <30) and marine aquatic environments listing sample origin and publication. (*): Daily rate based on 3 % conversion of ambient DON pool.

Samples	NH_4^+ photoproduction rates ($\text{nmol L}^{-1} \text{h}^{-1}$)	Reference
freshwater and estuarine filtered, isolated humics	50–370	Bushaw et al., 1996
freshwater	90	Gao and Zepp, 1998
freshwater	0	Jørgensen et al., 1998
freshwater	0	Bertilsson et al., 1999
freshwater filtered and ultrafiltered	110–4700	Wang et al., 2000
freshwater forest & agricultural runoff	0	Wiegner and Seitzinger, 2001
freshwater lake	763*	Vähätalo et al., 2003
coastal lake, salinity <4.4	–70–220	Gardner et al., 1998
estuarine isolated humics, salinity <25	7–60	Bushaw-Newton and Moran, 1999
estuarine filtered, coastal river plume	12–115	Morel and Corredor, 2001
freshwater, groundwater and estuarine, sal. <25	–294–34.8	Koopmans and Bronk, 2002
marine, coastal lagoon	1–46	Buffam and McGlathery, 2003
Eastern Tropical North Pacific	0.4–2.5	Bronk, 2002
open ocean	0.7–2.9	Present study

4 Discussion

4.1 Photoammonification

Table 3 compares photoammonification rates from the present study (not normalised for time-integrated irradiance in order to facilitate comparison) with previously published rates from a range of aquatic systems. The reported rate data (Table 3) span several orders of magnitude, presumably reflecting differences in DOM concentration and composition. Our photoammonification rate data from the oligotrophic Cyprus Gyre in the Eastern Mediterranean fall towards the low end of published rate data and are similar to those observed in other marine waters from the eastern tropical Pacific (Bronk, 2002). Other previous studies in coastal waters also found similar photoammonification rates for experimental procedures and light intensities comparable to those experienced in the Eastern Mediterranean during our work (e.g. Bushaw-Newton and Moran, 1999; Buffam and McGlathery, 2003). Freshwaters generally show up to 2 orders of magnitude higher rates of NH_4^+ photoproduction than do saline waters (Table 3). This finding may be attributed to the high DOM levels present in freshwaters, although other environmental variables including pH, iron and initial NH_4^+ concentration have also been shown to affect photoammonification. For example, ammonium photoproduction rates were shown to be correlated with photo-labile Fe concentration (Gao and Zepp, 1998) and inversely correlated with pH (Wang et al., 2000) and initial NH_4^+ (Koopmans and Bronk, 2002). River CDOM of up to 104 m^{-1} (e.g. Uher et al., 2001; Kowalczyk et al., 2003), DOC concentrations of $1200 \mu\text{mol L}^{-1}$ (e.g. Baker and Spencer, 2004), Fe and NH_4^+ concentrations of $2.3 \mu\text{mol L}^{-1}$ and $2.1 \mu\text{mol L}^{-1}$ respectively (e.g. Morris et

al., 1978) are typical for freshwaters. The occurrence of comparatively low photoammonification rates in the Cyprus gyre is therefore not unexpected given the low ambient DOM, Fe and NH_4^+ levels compared to those of typical freshwaters.

Our data from IREX 6 (Table 1) suggest that approximately 76% of total NH_4^+ photoproduction is attributable to UV light of wavelength $<360 \text{ nm}$, in broad agreement with previous work. By way of comparison, for irradiated freshwaters 47–83% of photoammonification was due to wavelengths $<360 \text{ nm}$ (Bushaw et al., 1996).

We found no evidence for light or dark NH_4^+ incorporation into DON during or after our irradiations, in contrast to the results of some other studies (Thorn and Mikita, 1992; Gardner et al., 1998; Koopmans and Bronk, 2002). Net photoconsumption of NH_4^+ has on occasion, been identified in both fresh and saline waters (Gardner et al., 1998; Koopmans and Bronk, 2002), while for other freshwaters NH_4^+ concentration changes remained undetectable (Jørgensen et al., 1998; Bertilsson et al., 1999; Wiegner and Seitzinger, 2001; Koopmans and Bronk, 2002). Koopmans and Bronk (2002) for example found net NH_4^+ uptake during the irradiation of groundwaters, with uptake rates inversely proportional to initial NH_4^+ concentration, consistent with the incorporation of NH_4^+ -N into DON as observed by Thorn and Mikita (1992) and Kieber et al. (1997). The contrast between these previous studies and consistent NH_4^+ photoproduction in all our samples presumably reflected DOM compositional variability related to DOM source, transformation history or differences in DOM and NH_4^+ concentrations.

Based on the notion that photochemical processes are largely affected by CDOM as indicated by its UV absorbance, photoammonification rates were frequently nor-

malised to a_{350} (Bushaw et al., 1996; Bushaw-Newton and Moran, 1999; Wang et al., 2000). Nevertheless, a recent compilation of available data on NH_4^+ photoproduction concluded that the variability in NH_4^+ photoproduction rates could not be attributed to variability in CDOM levels (Grzybowski, 2003). For our data from the Cyprus Gyre, we used the CDOM absorption coefficient at 300 nm, a_{300} , to test for possible CDOM-photoammonification relationships. In low CDOM oligotrophic marine waters, such as those in the Cyprus Gyre, the use of a_{300} is appropriate because the higher absorbance in the UV-B provides a better signal to noise ratio than that in the mid-UV (Kitidis et al., 2006). In agreement with Grzybowski (2003) our data did not support a direct correlation between photoammonification rates and CDOM (a_{350} or a_{300}). In addition no significant correlations were found between NH_4^+ photoproduction rates and other ancillary parameters such as DOC, DON, DOC:DON and initial NH_4^+ concentration. However, we found a significant correlation of NH_4^+ photoproduction rates with DOC normalised CDOM absorbance, a_{300} (Pearson correlation coefficient $R^2=0.52$, $p < 0.05$, $n=8$), i.e. higher photoammonification rates may be expected from more coloured ambient DOC. This may reflect prior sunlight exposure history and photobleaching of the ambient CDOM pool, in agreement with Buffam and McGlathery (2003) who reported that photoammonification rates in coastal seawater were correlated with rates of CDOM absorbance photobleaching at 280 nm. Preferential loss of CDOM compared to DOC has indeed been observed in long term irradiations of estuarine water (Moran et al., 2000). Photobleaching leads to accumulation of more photo-refractory CDOM with lower photobleaching rates and lower absorbance per unit carbon. Therefore the correlations of photoammonification rates with both photobleaching rates (Buffam and McGlathery, 2003) and DOC-normalised CDOM (this study), intrinsically link NH_4^+ photoproduction with prior radiation exposure.

CDOM photobleaching is likely responsible for the variations in DOC-normalised CDOM in our samples from the surface layer of the Cyprus Gyre. This contention is further corroborated by our finding that the distribution of DOC and a_{300} in our survey of the Cyprus Gyre clearly showed lower absorbance per unit carbon in near surface DOM (compared to deeper water in our study), presumably due to a photochemical CDOM sink in near surface waters. Similar findings were reported from the BATS station in the oligotrophic North Atlantic where the observed summer decrease in CDOM absorbance in the mixed layer was attributed to CDOM photo-oxidation (Siegel and Michaels, 1996). Decreasing CDOM:DOC ratios with distance offshore in the Mid Atlantic Bight were also ascribed to progressive CDOM photodegradation of terrestrial CDOM (Del Vecchio and Blough, 2004). Our data therefore suggest that regional differences in CDOM:DOC ratios may be of value in extrapolating photoammonification rates, although addi-

tional rate data on regional scales are needed to test this supposition.

4.2 Photochemical ammonium in the Cyprus Gyre

In order to estimate the annual rate of photoammonification in the Cyprus gyre, we scaled our apparent photoproduction rate estimates to take account of seasonal changes in solar irradiance, light attenuation by CDOM and surface mixed layer depth. Daily sea surface photoammonification (p_0) was first derived from our experimental photoproduction rate estimates and the proportion of daily irradiance received during the course of the irradiations from Eq. (2):

$$p_0 = (r \times \delta(t_{\text{ir.ex.}})) \times \frac{\int I t d(t)}{\int I t d(t_{\text{ir.ex.}})} \quad (2)$$

where r is the mean photoammonification rate, uncorrected for light intensity ($1.6 \text{ nmol L}^{-1} \text{ h}^{-1}$), $\delta(t_{\text{ir.ex.}})$ is the average duration of our irradiations, $\int I t d(t)$ is the daily ($t=0-24 \text{ h}$) integrated irradiance and $\int I t d(t_{\text{ir.ex.}})$ is the irradiance integrated over the average duration of the irradiation experiment. We used the rate obtained with Eq. (2) ($p_0=14.6 \text{ nmol L}^{-1} \text{ d}^{-1}$) to calculate the average photoammonification rate (p_z) in a water column of depth Z according to Eq. (3) as suggested by Moran and Zepp (2000):

$$p_z = \frac{p_0 \times (1 - e^{-k_d(\lambda) \times Z})}{Z \times K_d(\lambda)} \quad (3)$$

where $K_d(\lambda)$ is the light attenuation coefficient at wavelength λ . We calculated $K_d(\lambda)$ from the CDOM absorption coefficient according to Preisendorfer (1976),

$$K_d(\lambda) \approx \frac{4}{3} \times (a(\lambda) + a(\lambda)_w) \quad (4)$$

where $a(\lambda)$ and $a(\lambda)_w$ are the absorption coefficients of CDOM and pure water at wavelength λ respectively. Values for $a(\lambda)_w$ were obtained from Smith and Baker (1981). A small error is undoubtedly introduced by not measuring $K_d(\lambda)$ directly. However, recent work by Farmer et al. (1993) showed favourable agreement between $K_d(\lambda)$ observed in-situ and $K_d(\lambda)$ estimated from Eq. (4). Therefore, the major uncertainties in the calculations outlined above are the variability in photoammonification rates and the wavelength chosen to estimate the light attenuation coefficient. Wavelength dependence data for photoammonification are unavailable so far, but our data and those of Bushaw et al. (1996) show photoammonification to be dominated by wavelengths $< 360 \text{ nm}$. We therefore used $\lambda=300 \text{ nm}$ and $\lambda=350 \text{ nm}$ in order to define likely upper and lower constraints for K_d . The values derived from Eq. (4) were $K_d(300)=0.47 \text{ m}^{-1}$ and $K_d(350)=0.16 \text{ m}^{-1}$. Integrated over the euphotic layer (140 m deep), this yields corresponding p_z values of $174 \mu\text{mol m}^{-2} \text{ d}^{-1}$ and $302 \mu\text{mol m}^{-2} \text{ d}^{-1}$ for $K_d(300)$ and $K_d(350)$ respectively. Hence this procedure introduces an uncertainty of a factor of approximately 2 to our

estimate of p_z . Based on an estimated $K_d(330)=0.33\text{ m}^{-1}$ we calculate a daily euphotic layer depth-integrated photoammonification of $237\ \mu\text{mol m}^{-2}\text{ d}^{-1}$ in the euphotic layer.

Assuming our estimate of p_z to be typical for the Cyprus gyre in summer, we applied further seasonal corrections based on seasonal clear sky solar irradiance at 40° latitude (Leifer, 1988) averaged over the wavelength range from 300 to 800 nm. Dividing seasonal irradiance data by summer irradiance (Leifer, 1988) gave seasonal correction factors of 0.25, 0.75 and 0.43 for winter, spring, and autumn respectively (summer=1). A further correction factor for globally averaged cloud cover of 0.77 (Wayne, 2000) was applied. Annual photoammonification rate was then calculated from the sum of the respective seasonal contributions. The photochemical supply of NH_4^+ to the Cyprus gyre determined with this procedure is $40\pm 17\text{ mmol N m}^{-2}\text{ a}^{-1}$ (based on the mean photoammonification rate \pm standard deviation from our experiments). This value is of the same order of magnitude as the estimated inorganic N supply to the eastern Mediterranean through atmospheric deposition, $71\text{ mmol N m}^{-2}\text{ a}^{-1}$ (Herut et al., 1999, 2002), and corresponds to $12\pm 5\%$ of the annual nitrogen demand for new production in the Cyprus Gyre (Krom et al. 1992). Therefore, our preliminary estimate of water-column photoammonification clearly indicates a potentially significant contribution of photochemical NH_4^+ release to the N budget of the Cyprus Gyre region. As the Cyprus Gyre undergoes episodes of P-limitation the overall impact of photochemical NH_4^+ release on primary production may in part be controlled by the availability of P. Although PO_4^{3-} addition had no effect on NH_4^+ photoproduction rates during our study, it would affect the biological uptake of photoproduced NH_4^+ since primary producers are thought to be P-limited in the study area. Onboard microcosm experiments during which NH_4^+ was added to IN-patch water samples after P-release showed increased bacterial activity (measured as ^{14}C -leucine incorporation) and a 4–80 fold increase in chlorophyll compared to OUT-patch control treatments and IN-patch samples without added P (Zohary et al., 2005). These results indicate that, under similar situations, photochemically released NH_4^+ is likely to stimulate phytoplankton production in the presence of sufficient P. Further studies of photochemical NH_4^+ release in the open ocean will help to constrain more tightly, the role of photoammonification in oligotrophic marine ecosystems.

5 Conclusions

In this study we describe the first dataset on photoammonification from an oligotrophic open ocean environment (Cyprus Gyre, Eastern Mediterranean). This process is related to the chromophoric content of dissolved organic matter (DOM) and its photodegradation, largely through UV radiation. Ammonium (NH_4^+) photochemical production has the potential to significantly impact on the biogeochemical cycling of ni-

trogen (N) in the marine environment, as a source of bioavailable N. In the case of the Eastern Mediterranean, our preliminary calculations show that this process is of the same order of magnitude as previously calculated atmospheric N deposition. Furthermore, photoammonification is expected to drive the Eastern Mediterranean further towards phosphorous limitation. It is therefore apparent that the current omission of this process from marine biogeochemical ecosystem models should be addressed. This requires additional field and experimental data, in particular extending the geographic and seasonal data coverage and improving our understanding of the wavelength dependence of photoammonification. A further requirement of future work is to explore the environmental controls of photoammonification and assess the impact of DOM quality and source (marine, terrestrial or anthropogenic) through molecular characterisation of DOM. The latter is particularly important for the Eastern Mediterranean due to its enclosed nature and increased pressures from a growing human population.

Acknowledgements. The authors would like to thank M. Krom and the EU CYCLOPS scientific community as well as the captain and crew of R. V. *Aegaeo*. Specifically we would like to thank A. Rees for assistance with sampling, M. Zubkov for flow cytometry analyses, S. Groom and the Plymouth Marine Laboratory Remote Sensing Data Analysis Service for providing the SeaWiFS image of the study area. We would also like to thank three anonymous reviewers for their constructive criticism of this manuscript. This work was funded by the Natural Environment Research Council of the UK (grant number: NER/B/S/2001/00913).

Edited by: T. W. Lyons

References

- Alvarez-Salgado, X. A. and Miller, A. E. J.: Simultaneous determination of dissolved organic carbon and total dissolved nitrogen in seawater by high temperature catalytic oxidation: conditions for precise shipboard measurements, *Mar. Chem.*, 62(3–4), 325–333, 1998.
- Baker, A. and Spencer, R. G. M.: Characterization of dissolved organic matter from source to sea using fluorescence and absorbance spectroscopy, *Sci. Total Environ.*, 333(1–3), 217–232, 2004.
- Bertilsson, S., Stepanauskas, R., Cuadros-Hansson, R., Graneli, W., Wikner J., and Tranvik, L.: Photochemically induced changes in bioavailable carbon and nitrogen pools in a boreal watershed, *Aquatic Microbial Ecology*, 19, 47–56, 1999.
- Brewer, P. G. and Riley J. P.: The automatic determination of nitrate in sea water, *Deep-Sea Res.*, 12, 765–772, 1965.
- Bronk, D. A.: Dynamics of DON, in: *Biogeochemistry of Marine Dissolved Organic Matter*, edited by: Hansell D. A. and Carlson, C. A., Academic Press, London, 2002.
- Buffam, I. and McGlathery, K. J.: Effect of ultraviolet light on dissolved nitrogen transformations in coastal lagoon water, *Limnology and Oceanography*, 48(2), 723–734, 2003.
- Bushaw, K. L., Zepp, R. G., Tarr, M. A., Shulz-Jander, D., Bourbonniere, R. A., Hodson, R. E., Miller, W. L., Bronk, D. A.,

- and Moran, M. A.: Photochemical release of biologically available nitrogen from aquatic dissolved organic matter, *Nature*, 381, 404–407, 1996.
- Bushaw-Newton, K. L. and Moran, M. A.: Photochemical formation of biologically available nitrogen from dissolved humic substances in coastal marine systems, *Aquatic Microbial Ecology*, 18, 285–292, 1999.
- Farmer, C. T., Moore, C. A., Zika, R. G., and Sikorski, R. J.: Effects of Low and High Orinoco River Flow on the Underwater Light Field of the Eastern Caribbean Basin, *J. Geophys. Res.*, 98, 2279–2288, 1993.
- Gao, H. and Zepp, R. G.: Factors Influencing Photoreactions of Dissolved Organic Matter in a Coastal River of the Southeastern United States, *Environ. Sci. Technol.*, 32, 2940–2946, 1998.
- Gardner, W. S., Cavaletto, J. F., Bootsma, H. A., Lavrentyev, P. J., and Troncone, F.: Nitrogen cycling rates and light effects in tropical Lake Maracaibo, Venezuela, *Limnology and Oceanography*, 43(8), 1814–1825, 1998.
- Goeyens, L., Kindermans, N., Yusuf, M. A., and Elskens, M.: A Room Temperature Procedure for the Manual Determination of Urea in Seawater, *Estuarine Coastal and Shelf Science*, 47, 415–418, 1998.
- Grasshoff, K.: Determination of Nitrite, in: *Methods of Seawater Analysis*, edited by: Grasshoff, K., Ehrhardt, M., and Kremling, K., Weinheim, Verlag Chemie, 139–142, 1983.
- Green, S. A. and Blough, N. V.: Optical absorption and fluorescence properties of chromophoric dissolved organic matter in natural waters, *Limnology and Oceanography*, 39(8), 1903001916, 1994.
- Grzybowski, W.: Are data on light-induced ammonium release from dissolved organic matter consistent?, *Chemosphere*, 52, 93300936, 2003.
- Herut, B., Krom, M. D., Pan, G., and Mortimer, R.: Atmospheric input of nitrogen and phosphorus to the Southeast Mediterranean: Sources, fluxes and possible impact, *Limnology and Oceanography*, 44(7), 1683001692, 1999.
- Herut, B., Collier, R., and Krom, M. D.: The role of dust in supplying nitrogen and phosphorus to the southeast Mediterranean, *Limnology and Oceanography*, 47(3), 87000878, 2002.
- Jones, R. D.: An improved fluorescence method for the determination of nanomolar concentrations of ammonium in natural waters, *Limnology and Oceanography*, 36(4), 814–819, 1991.
- Jørgensen, N. O. G., Tranvik, L., Edling, H., Graneli, W., and Lindell, M.: Effects of sunlight on occurrence and bacterial turnover of specific carbon and nitrogen compounds in lake water, *FEMS Microbiol. Ecol.*, 25, 217–227, 1998.
- Kieber, R. J., Hydro, L. H., and Seaton, P. J.: Photooxidation of triglycerides and fatty acids in seawater: Implications toward the formation of marine humic substances, *Limnology and Oceanography*, 42(6), 1454–1462, 1997.
- Kieber, R. J., Li, A., and Seaton, P. J.: Production of Nitrite from the Photodegradation of Dissolved Organic Matter in Natural Waters, *Environ. Sci. Technol.*, 33, 993–998, 1999.
- Kitidis, V.: CDOM dynamics and photoammonification in the marine environment, Ph.D. Thesis, University of Newcastle, p. 182, 2002.
- Kitidis, V., Stubbins, A. P., Uher, G., Upstill-Goddard, R., Law, C. S., and Woodward, E. M. S.: Variability of Chromophoric Organic Matter in surface waters of the Atlantic Ocean, *Deep Sea Res. II*, 53, 1666–1684, 2006.
- Koopmans, D. J. and Bronk, D. A.: Photochemical production of dissolved inorganic nitrogen and primary amines from dissolved organic nitrogen in waters of two estuaries and adjacent surficial groundwaters, *Aquatic Microbial Ecology*, 26, 295–304, 2002.
- Kowalczyk, P., Cooper, W. J., Whitehead, R. F., Durako, M. J., and Sheldon, W.: Characterization of CDOM in an organic-rich river and surrounding coastal ocean in the South Atlantic Bight, *Aquatic Sciences*, 65(4), 384–401, 2003.
- Krom, M. D., Kress, N., Brenner, S., and Gordon, L. I.: Phosphorus limitation of primary productivity in the eastern Mediterranean Sea, *Limnology and Oceanography*, 36(3), 424–432, 1991.
- Krom, M. D., Brenner, S., Kress, N., Neori, A., and Gordon, L. I.: Nutrient dynamics and new production in a warm-core eddy from the Eastern Mediterranean Sea, *Deep Sea Res. I*, 39(3/4), 467–480, 1992.
- Krom, M. D., Thingstad, T. F., Brenner, S., Carbo, P., Drakopoulos, P., Fileman, T. W., Flaten, G. A. F., Groom, S., Herut, B., Kitidis, V., Kress, N., Law, C. S., Liddicoat, M. I., Mantoura, R. F. C., Pasternak, A., Pitta, P., Polychronaki, T., Psarra, S., Rassoulzadegan, F., Skjoldal, E. F., Spyres, G., Tanaka, T., Tselepidis, A., Wassmann, P., Riser, C. W., Woodward, E. M. S., Zodiatis, G., and Zohary, T.: Summary and overview of the CYCLOPS P addition Lagrangian experiment in the Eastern Mediterranean, *Deep Sea Res. II*, 52, 3090–3108, 2005a.
- Krom, M. D., Woodward, E. M. S., Herut, B., Kress, N., Carbo, P., Mantoura, R. F. C., Spyres, G., Thingstad, T. F., Wassmann, P., Wexels-Riser, C., Kitidis, V., Law, C. S., and Zodiatis, G.: Nutrient cycling in the south east Levantine basin of the eastern Mediterranean: Results from a phosphorus starved system, *Deep Sea Res. II*, 52, 2879–2896, 2005b.
- Law, C. S., Abraham, E. R., Woodward, E. M. S., Liddicoat, M. I., Fileman, T. W., Thingstad, T. F., Kitidis, V., and Zohary, T.: The fate of Phosphate in a Lagrangian enrichment experiment in the Eastern Mediterranean, *Deep Sea Res. II*, 52, 2911–2927, 2005.
- Leifer, A.: *The kinetics of environmental aquatic photochemistry: Theory and Practice*, American Chemical Society, 1988.
- Moran, M. A., Sheldon, W. M., and Zepp, R. G.: Carbon loss and optical property changes during long-term photochemical and biological degradation of estuarine dissolved organic matter, *Limnology and Oceanography*, 45, 1254–1264, 2000.
- Moran, M. A. and Zepp, R. G.: UV radiation effects on microbes and microbial processes, in: *Microbial Ecology of the Oceans*, edited by: Kirchman D. L., John Wiley & Sons Ltd., New York, 2000.
- Morell, J. M. and Corredor, J. E.: Photomineralization of fluorescent organic matter in the Orinoco River plume: Estimation of ammonium release, *J. Geophys. Res.-Oceans*, 106(C8), 16 807–16 813, 2001.
- Pegau, W. S. and Zaneveld, J. R. V.: Temperature-Dependent Absorption of Water in the Red and near-Infrared Portions of the Spectrum, *Limnology and Oceanography*, 38, 188–192, 1993.
- Preisendorfer, R. W.: *Hydrologic Optics*, Vol. 5, U.S. Department of Commerce, NOAA Environmental Research Laboratory, Washington D.C., 1976.
- Rees, A., Woodward, M., and Joint, I.: Measurement of nitrate and ammonium uptake at ambient concentrations in oligotrophic waters of the North-East Atlantic Ocean, *Marine Ecology Progress Series*, 187, 295–300, 1999.

- Siegel, D. A. and Michaels, A. F.: Quantification of non-algal light attenuation in the Sargasso Sea: Implications for biogeochemistry and remote sensing, *Deep Sea Res. II*, 43, 321–345, 1996.
- Smith, R. C. and Baker, K. S.: Optical properties of the clearest natural waters (200–800 nm), *Appl. Opt.*, 20, 177–184, 1981.
- Spokes, L. J. and Liss, P. S.: Photochemically induced redox reactions in seawater, II. Nitrogen and iodine, *Mar. Chem.*, 54, 1–10, 1996.
- Spyres, G., Nimmo, M., Worsfold, P. J., Achterberg, E. P., and Miller, A.E.J.: Determination of dissolved organic carbon in seawater using high temperature catalytic oxidation techniques. *Trac-Trends in Analytical Chemistry*, 19, 498–506, 2000.
- Tarr, M., Wang, W., Bianchi, T. S., and Engelhaupt, E.: Mechanisms of ammonia and amino acid photoproduction from aquatic humic and colloidal matter, *Water Res.*, 35(15), 3688–3696, 2001.
- Thingstad, T. F., Krom, M. D., Mantoura, R. F. C., Flaten, G. A. F., Groom, S., Herut, B., Kress, N., Law, C. S., Pasternak, A., Pitta, P., Psarra, S., Rassoulzadegan, F., Tanaka, T., Tselepidis, A., Wassmann, P., Woodward, E. M. S., Riser, C. W., Zodiatis, G., and Zohary, T.: Nature of phosphorus limitation in the ultra-oligotrophic eastern Mediterranean, *Science*, 309, 1068–1071, 2005.
- Thorn, K. A. and Mikita, M. A.: Ammonia fixation by humic substances: a nitrogen-15 and carbon-13 NMR study, *Sci. Total Environ.*, 113, 67–87, 1992.
- Uher, G., Hughes, C., Henry, G., and Upstill-Goddard, R. C.: Non-conservative mixing behavior of colored dissolved organic matter in a humic-rich, turbid estuary, *Geophys. Res. Lett.*, 28, 3309–3312, 2001.
- Vähätalo, A. V., Salonen, K., Muenster, U., Jarvinen, M., and Wetzel, R. G.: Photochemical transformation of allochthonous organic matter provides bioavailable nutrients in a humic lake, *Archiv für Hydrobiologie*, 156(3), 287–314, 2003.
- Wayne, R. P.: *Chemistry of Atmospheres*, Oxford University Press, Oxford, 2000.
- Wang, W., Tarr, M. A., Bianchi, T. S., and Engelhaupt, E.: Ammonium Photoproduction from Aquatic Humic and Colloidal Matter, *Aquatic Geochemistry*, 6, 275–292, 2000.
- Wiegner, T. N. and Seitzinger, S. P.: Photochemical and microbial degradation of external dissolved organic matter inputs to rivers, *Aquatic Microbial Ecology*, 24, 27–40, 2001.
- Zohary, T., Herut, B., Krom, M. D., Mantoura, R. F. C., Pitta, P., Psarra, S., Rassoulzadegan, F., Stambler, N., Tanaka, T., Thingstad, T. F., and Woodward, E. M. S.: Is the Eastern Mediterranean N & P co-limited in summer? The response of P supplemented water to added ammonia in an on-board microcosm experiment, *Deep Sea Res. II*, 52, 3024–3040, 2005.